

Oscillations and quantized second-harmonic generation

Craig M. Savage

Optical Sciences Center, University of Arizona, Tucson, Arizona 85721

(Received 27 April 1987)

We investigate quantum-mechanical second-harmonic generation for parameters such that classical electrodynamics predicts oscillations. Specifically we calculate the Q distribution function in a Gaussian approximation about the classical limit cycle. In the classical limit initial rapid collapse of the Q distribution into the neighborhood of the limit cycle is followed by diffusion around the limit cycle. The experimental significance of this quantum diffusion is discussed.

Second-harmonic generation in a driven optical cavity is a particularly suitable system for investigating the interface between quantum and classical dynamics. Classical electrodynamics predicts a range of behaviors including self-pulsing,¹ which has recently been observed,² and period doubling sequences to chaos.³ This variety is produced by a quadratic nonlinear coupling of the subharmonic and second-harmonic modes. Currently there is much interest in how such dynamics, especially chaos, can be described within the framework of quantum mechanics.^{4,5} In the following we show for the example of second-harmonic generation that the quantum dynamics associated with classical oscillations is physically straightforward. In the "classical limit" of large fields and small nonlinearity the quantum dynamics reduces to classical Liouville dynamics plus classical noise. Though reasonable this result is not immediate from the Fokker-Planck-type equation obeyed by the Q distribution since its diffusion matrix need not be positive semidefinite anywhere on the limit cycle.

In order to obtain everywhere positive semidefinite diffusion one uses the Fokker-Planck equation for the positive P representation of Drummond and Gardiner.⁶ This has the advantage of being equivalent to a system of stochastic differential equations in a phase space of double the classical phase-space dimension.⁷ Dörfle and Schenzle⁸ have recently analyzed the attractors of the deterministic part of these equations in this "doubled dimension" phase space. They found that corresponding to a classical limit cycle attractor is an attracting two-dimensional manifold that may be pictured as a topological cylinder of limit cycles stacked into the extra "non-physical" dimensions. Furthermore, this manifold is noncompact so that individual stochastic differential equation trajectories may diffuse off to infinity. Hence, a stationary positive P representation does not exist. The physical significance of this, if any, is presently unclear.

Dörfle and Graham⁹ have presented preliminary work using the dynamical equation for the Wigner function for second-harmonic generation. It contains third-order derivatives which they ignore and subsequently approximate the system in the classical limit by the remaining Fokker-Planck equation. We retain all terms in our dynamical equation for the Q distribution.

Other quantum-mechanical systems whose classical counterparts show oscillations have been studied. Graham has recently presented a summary of work on quantum maps¹⁰ and has also reported that the stationary Wigner function for the quantized Lorenz model reduces to the classical invariant measure in the classical limit.¹¹ Graham and Tel¹² have constructed approximate stationary distributions for systems having deterministic limit cycles. Satchell and Sarkar¹³ have used a computationally intensive method to analyze the oscillatory solutions of an anharmonic oscillator with a time-dependent interaction Hamiltonian. The present work does not deal with the stationary behavior and has a time-independent Hamiltonian. Since the phase space of second-harmonic generation has two complex, or four real, dimensions it would be very expensive to solve numerically by the method of Satchell and Sarkar.¹³ The technique of Gaussian approximation around the classical-trajectory point reduces the numerical burden enormously.

The density operator ρ for intracavity second-harmonic generation (SHG) satisfies the master equation⁷

$$\frac{d\rho}{dt} = (i\hbar)^{-1}[H, \rho] + \sum_{i=1}^2 \gamma_i (2a_i \rho a_i^\dagger - a_i^\dagger a_i \rho - \rho a_i^\dagger a_i). \tag{1}$$

Subscripts 1 and 2 refer to the subharmonic and second-harmonic cavity modes, respectively and a_i^\dagger, a_i are their boson creation and annihilation operators. The first term contains the interaction Hamiltonian H defined by

$$(i\hbar)^{-1}H = \sum_{i=1}^2 -i\Delta_i a_i^\dagger a_i + E(a_1^\dagger - a_1) + \frac{1}{2}\chi(a_1^\dagger a_2 - a_2^\dagger a_1), \tag{2}$$

where Δ_i is the cavity detuning of mode i , E is the subharmonic driving field amplitude, and χ the nonlinear susceptibility responsible for the second-harmonic generation. The final two terms in Eq. (1) describe the damping of the modes at rate γ_i . We note that the amplitude coupling to the reservoirs which leads to this

form of damping generates approximate continuous "measurements" of the complex amplitudes a_1 and a_2 ,¹⁴ a point we will return to later.

In order to obtain a c -number equation equivalent to the operator master equation (1) a variety of quasiprobability distributions may be introduced.¹⁵ We shall use the Q distribution function, defined as the diagonal matrix elements of the density operator ρ in the coherent state basis,

$$Q(\alpha_1, \alpha_2) = (\langle \alpha_1 | \otimes \langle \alpha_2 | \rho | \alpha_1 \rangle \otimes | \alpha_2 \rangle). \quad (3)$$

where $|\alpha_i\rangle$ is the coherent state with complex amplitude α_i of mode i . From this definition it follows that $\pi^{-2}Q(\alpha_1, \alpha_2)$ is a genuine probability distribution satisfying

$$0 \leq Q(\alpha_1, \alpha_2) \leq 1, \quad (4a)$$

$$\pi^{-2} \int \int Q(\alpha_1, \alpha_2) d^2\alpha_1 d^2\alpha_2 = 1. \quad (4b)$$

These important features distinguish the Q distribution from other representations, such as the Glauber-Sudarshan P representation, which may become negative and indeed highly singular. Thus the Q distribution is suited to our Gaussian approximation method.

In a sense made precise by Davis,¹⁶ $\pi^{-2}Q(\alpha_1, \alpha_2)$ is the probability distribution for measuring the complex amplitudes α_1, α_2 to the accuracy allowed by the uncertainty principle resulting from the boson commutation relation. This physical interpretation will be important in our discussion of the classical limit of SHG. Millburn⁷ has used the Q distribution to analyze the quantum and classical dynamics of the anharmonic oscillator and we refer to that paper for further discussion of its interpretation.

After normal ordering and using $[a^\dagger, \rho] = -\partial_a \rho$ and its Hermitean conjugate we find that Eq. (1) implies that the Q distribution satisfies¹⁸

$$\partial_\tau Q(\alpha, \tau) = [-\partial_i b^i + \frac{1}{2}(\chi/\gamma_1)^2 \partial_i \partial_j d^{ij}] Q(\alpha, \tau), \quad (5a)$$

$$b^1 = -\alpha_{1r} + \Delta'_1 \alpha_{1i} + \alpha_{1r} \alpha_{2r} + \alpha_{1i} \alpha_{2i} + E', \quad (5b)$$

$$b^2 = -\alpha_{1i} - \Delta'_1 \alpha_{1r} + \alpha_{1r} \alpha_{2i} - \alpha_{1i} \alpha_{2r}, \quad (5c)$$

$$b^3 = -\gamma' \alpha_{2r} + \Delta'_2 \alpha_{2i} - \frac{1}{2}(\alpha_{1r}^2 - \alpha_{1i}^2), \quad (5d)$$

$$b^4 = -\gamma' \alpha_{2i} - \Delta'_2 \alpha_{2r} - \alpha_{1r} \alpha_{1i}, \quad (5e)$$

$$d^{11} = 1 - \frac{1}{2} \alpha_{2r}, \quad d^{22} = 1 + \frac{1}{2} \alpha_{2r}, \quad (5f)$$

$$d^{12} = d^{21} = -\frac{1}{2} \alpha_{2i}, \quad d^{33} = d^{44} = \gamma', \quad (5g)$$

$$\alpha^T = (\alpha_{1r}, \alpha_{1i}, \alpha_{2r}, \alpha_{2i}), \quad (5g)$$

$$\tau = \gamma_1 t, \quad \Delta'_i = \frac{\Delta_i}{\gamma_1}, \quad \gamma' = \frac{\gamma_2}{\gamma_1}, \quad E' = \frac{E\chi}{\gamma_1^2}. \quad (5h)$$

We refer to the b^i as the drift coefficients and to the d^{ij} as the diffusion matrix elements, and all those not explicitly assigned a value are zero. The subscripts and superscripts i and j refer to the elements of the vector (5g) which are scaled real and imaginary parts of the complex field amplitudes defined by

$$\begin{aligned} \alpha_1 &= (\chi/\gamma_1)^{-1} (\alpha_{1r} + i\alpha_{1i}), \\ \alpha_2 &= (\chi/\gamma_1)^{-1} (\alpha_{2r} + i\alpha_{2i}). \end{aligned} \quad (6)$$

Since it is a function of scaled amplitudes the Q distribution of Eq. (5a) is of course also scaled relative to that of Eq. (3). At this point we note that the eigenvalues of the diffusion matrix d^{ij} are

$$\lambda' = \gamma', \gamma', 1 + \frac{1}{2} |\alpha_2|, 1 - \frac{1}{2} |\alpha_2|,$$

and so it is negative definite whenever $|\alpha_2| > 2$ (Fig. 1). The limit $\chi/\gamma_1 \rightarrow 0$ (or similarly $\chi/\gamma_2 \rightarrow 0$) is a natural classical limit for SHG because the diffusion term in Eq. (5a) goes to zero in this limit. From Eqs. (6) this is the large-field limit, and physically large fields and small nonlinearity are expected to be well described by classical electrodynamics. For long enough times even small quantum diffusion will become significant so we also expect the classical limit to be a short-time limit. Of course, the quantum-mechanical uncertainty principles require a minimum phase-space volume, even in the classical limit, and so we are considering classical Liouville dynamics.

After making the usual approximations Maxwell's classical theory gives the following equations for the classical field amplitudes:^{19,1}

$$\frac{d\alpha_{1r}}{d\tau} = b^1, \quad \frac{d\alpha_{1i}}{d\tau} = b^2, \quad \frac{d\alpha_{2r}}{d\tau} = b^3, \quad \frac{d\alpha_{2i}}{d\tau} = b^4, \quad (7)$$

where the b^i are defined in Eqs. 5(b)–5(e). These are the equations for the characteristics of the first-order part of Eq. 5(a). So if the diffusion part of the Q distribution equation (5a) were zero it would be the classical Liouville equation. In the classical limit of small diffusion we expect the diffusion terms to be a small perturbation of

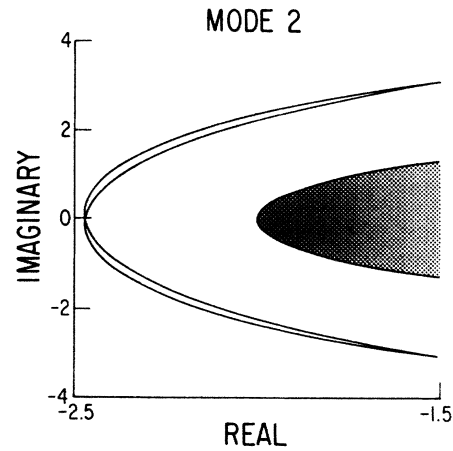


FIG. 1. Limit cycle of Eqs. (7), α_{2r} vs α_{2i} , defined by Eq. (6) as dimensionless scaled real and imaginary parts of the complex field amplitude of mode 2. Parameters: $E' = 11.11$, $\Delta'_1 = \Delta'_2 = 0$, $\gamma' = 1$, period $\cong 2.312\gamma_1^{-1}$. Diffusion matrix D is positive semidefinite only inside the shaded area. Note the different scales on the axes.

the classical solution defined by Eqs. (7). Thus in the classical limit we associate the quantum Q distribution arguments with the classical field amplitudes.

Equation 5(a) may be solved in the classical limit $\chi/\gamma_1 \rightarrow 0$ by making the ansatz²⁰

$$Q(\alpha, \tau) = z(\alpha, \tau) \exp[-2(\chi/\gamma_1)^{-2} \phi(\alpha, \tau)]. \quad (8)$$

Substituting this into Eq. 5(a) we find to highest order in $(\chi/\gamma_1)^{-1}$,¹³

$$\partial_\tau \phi + b^i \phi_i + \frac{1}{2} d^{ij} \phi_i \phi_j = 0, \quad (9)$$

where the subscripts denote partial differentiation with respect to the vector elements of Eq. (5g) and summation is implied by repeated indices. Following Ludwig²¹ and Kubo *et al.*²² we now expand ϕ and the b^i about the deterministic trajectory $\alpha_d(\tau)$ which solves Eqs. (7).

$$\begin{aligned} \phi(\alpha, \tau) &= \phi(\alpha_d + \delta\alpha, \tau) \\ &= \phi_i(\tau) \delta\alpha^i + \frac{1}{2} \phi_{ij}(\tau) \delta\alpha^i \delta\alpha^j + \dots, \end{aligned} \quad (10a)$$

$$b^i(\alpha, \tau) = b^i(\alpha_d + \delta\alpha, \tau) = b_0^i(\tau) + b_k^i \delta\alpha^k + \dots, \quad (10b)$$

where we have noted $\phi(\alpha_d(\tau), \tau) = 0$.²¹ Substituting in Eq. (9) and equating the terms constant, linear, and quadratic in $\delta\alpha$ separately to zero, we find

$$\phi_i = 0, \quad (11a)$$

$$\phi_{i\tau} + b^k \phi_{ki} = 0, \quad (11b)$$

$$\phi_{ij\tau} + b^k \phi_{ijk} + b_i^k \phi_{kj} + d^{kl} \phi_{ki} \phi_{lj} = 0. \quad (11c)$$

Due to Eq. (11a) our Gaussian approximation to the Q distribution will be centered on the deterministic trajectory, while Eq. (11b) confirms that ϕ_i is constant along the deterministic trajectory. The final equation (11c) can be written in the matrix form

$$\frac{d}{d\tau} \Phi + \Phi \mathbf{B} + \mathbf{B}^T \Phi + \Phi \mathbf{D} \Phi = 0, \quad (12a)$$

$$\Phi_{ij} = \phi_{ij}, \mathbf{B}_{ij} = b_j^i, \mathbf{D}_{ij} = d^{ij}, \quad (12b)$$

where the derivative is along the deterministic trajectory, parametrized by time, and we have explicitly assured the symmetry of Φ . The linearized drift matrix \mathbf{B} and diffusion matrix \mathbf{D} must be evaluated along a deterministic trajectory defined by Eqs. (7). Hence, coupling the 20, first-order, nonlinear, ordinary differential equations (7) and (12a) together we can numerically solve for the ϕ_{ij} .

It can be shown that the coefficient $z(\alpha, \tau)$ in Eq. (8) is²¹

$$z(\alpha, \tau) = c \det[\Phi]^{1/2}, \quad (13)$$

with c a normalization constant. So our Gaussian approximation to the Q distribution, valid for $\chi/\gamma_1 \rightarrow 0$ and near the deterministic trajectory point $(\alpha_d(\tau), \tau)$, is

$$Q(\alpha, \tau) \cong c \det[\Phi]^{1/2} \exp[-2(\chi/\gamma_1)^{-2} \delta\alpha^T \Phi \delta\alpha], \quad (14a)$$

$$\delta\alpha = \alpha - \alpha_d(\tau), \quad (14b)$$

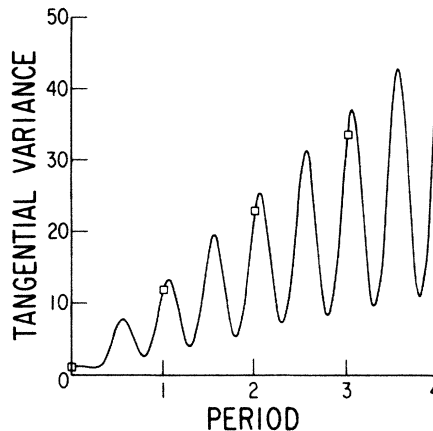


FIG. 2. Tangential variance $\delta\alpha_i^T \Phi \delta\alpha_i$ (dimensionless), where $\delta\alpha_i$ is the unit vector tangential to the deterministic trajectory, vs time, in units of the period, for limit cycle of Fig. 1. The boxes mark the same point on the limit cycle. Note the linear growth from period to period.

where Φ is to be calculated numerically. That our approximation Eq. (14a) is valid only near a trajectory point $(\alpha_d(\tau), \tau)$ limits its application to times sufficiently short that significant diffusion away from this point has not occurred. The method of Gaussian approximation just presented is equivalent to the moment expansion described by van Kampen.²³ For further discussion of this relationship see Kubo *et al.*²²

Our interest is in parameters for which the classical system, Eqs. (7), has an attracting limit cycle on which the diffusion matrix \mathbf{D} is everywhere nonpositive semidefinite e.g., Fig. 1. When the detunings Δ_1, Δ_2 are zero the dynamical system, Eqs. (7), is invariant under complex conjugation, which accounts for the symmetry

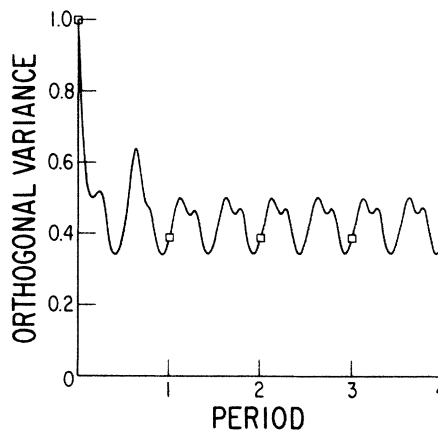


FIG. 3. Orthogonal variance $\delta\alpha_0^T \Phi \delta\alpha_0$ vs time for limit cycle of Fig. 1. The curve is for $\delta\alpha_0$ orthogonal to the limit cycle tangent vector. Specifically $\delta\alpha_0 = i - [i \cdot \delta\alpha_i] \delta\alpha_i$, where i has components $\alpha_{1r} = 1, \alpha_{1i} = \alpha_{2r} = \alpha_{2i} = 0$. Other orthogonal variances behave similarly. Note the variance axis range is $\frac{1}{50}$ that of Fig. 2.

under reflection in the real axis of the projected limit cycle, Fig. 1. We note that analytic approximations for the limit cycles, valid near the Hopf bifurcation point, have been presented.²⁴ We solve the system of equations (7) and (12a) for an initial coherent state on the limit cycle so that Φ is initially the identity matrix and the (scaled) initial variances are $\frac{1}{4}(\chi/\gamma_1)^2$. In Fig. 2 we have plotted the variances $\delta\alpha^T\Phi\delta\alpha$ versus time for $\delta\alpha$ tangential to the limit cycle and in Fig. 3 for a direction orthogonal to the limit cycle.

The important point illustrated by these graphs of the variances concerns their behavior at a fixed, but arbitrary, phase-space point on the limit cycle from one period to the next. Such a point is marked by the boxes in the figures. The tangential variance, Fig. 2, grows linearly from period to period while the orthogonal variance, Fig. 3, quickly reaches a small value which is constant from period to period. Having made these essential observations we now clarify some details of the graphs. The previously mentioned symmetry of the dynamical system under complex conjugation accounts for the underlying periodicity of the variances being half the limit cycle period. The behavior of the variances within a period follows, of course, from the details of the variation of the drift and diffusion around the limit cycle. Also the particular orthogonal variance plotted is a function not only of the dynamics but also of the particular choice of orthogonal direction from the three-dimensional orthogonal subspace, which is different for different tangent vectors.

We have previously mentioned that $Q(\alpha_1, \alpha_2)$ may be interpreted as the probability distribution for "measuring" the complex amplitudes α_1, α_2 . Now the observables corresponding to the real and imaginary parts of α_i do not commute, so the measurement of α_i will be limited by the uncertainty principle resulting from the boson commutation relation. It is thus in a generalized sense that we refer to a measurement of the non-Hermitian operator α_i .^{14,16,17} With this understanding Fig. 3 may be interpreted as showing that if we start with initial coherent states $|\alpha_1\rangle \otimes |\alpha_2\rangle$ on the classical limit cycle and measure the coherent amplitudes after about a period we will find them to be concentrated on the classical limit cycle. From Fig. 2 we see that the tangential variance about the deterministic amplitude, at a particular trajectory point, increases linearly with time. According to Eq. (14a) the variances scale as $(\chi/\gamma_1)^2$ so that in the classical limit, $\chi/\gamma_1 \rightarrow 0$, the orthogonal spreading and the rate of tangential spreading, as proportions of the unscaled amplitudes, both approach zero. This very reasonable description would be expected if the classical dynamical system Eq. (7) were perturbed by classical noise.²⁵ However, this does not follow immediately from the Q distribution dynamical equation (5a) since the diffusion matrix \mathbf{D} is nowhere positive

semidefinite on the deterministic limit cycle in the current example, Fig. 1. Although our Gaussian approximation cannot describe the stationary state it is consistent with the expectation that diffusion around the entire limit cycle occurs, as found by Graham,¹¹ for the quantized Lorentz attractor.

It is important to realize that although the probability distribution for measuring the complex amplitudes is governed by the classical equations, in the classical limit, quantum phenomena such as squeezing^{2,26,27} may still be present. This is a manifestation of the fundamental quantum-mechanical nature of the system which may be probed by making appropriate measurements, such as of the squeezing. This fundamental quantum nature is ensured by the strictly different interpretation of the Q distribution arguments and the classical complex amplitudes. Nevertheless, the complex amplitudes behave classically over short enough times in the limit $\chi/\gamma_1 \rightarrow 0$. In order to understand why it is the complex amplitudes that behave classically we note that the damping in Eq. (1) acts like a continuous measurement of the complex amplitudes insofar as it tends to diagonalize the density matrix in the coherent-state basis.^{14,28} That the particular measurements made on a system may be important in determining its classical limit has been emphasized by Lamb²⁹ and recently by Meystre and Wright.³⁰

Consider an experiment having $\gamma_1 = \gamma_2 = 20$ MHz and $\chi = 10$ kHz so that $\chi/\gamma_1 = 5 \times 10^{-4}$ and the oscillation frequency is roughly $\sqrt{3}\gamma_1/2\pi = 6$ MHz.^{1,2} From Fig. 2 we see that the tangential variance is increasing by about $10(\chi/\gamma_1)^2$ per period and thus will reach unity after about 4×10^5 periods or 60 msec, assuming tangential diffusion to continue at the rate given by the Gaussian approximation. Hence, if other technical sources of noise disturbed the oscillation phase by much less than a period over 60 msec one might hope to see the fundamental quantum phase diffusion as a broadening of order 10 Hz on the 6-MHz oscillation signal. Increasing the ratio χ/γ_1 will increase the broadening.

In summary we have calculated the "quantum diffusion" correction to the classical periodic oscillations that occur in second-harmonic generation. These quantum corrections only become important for times so long that it may be difficult to detect them in current experiments against the background of technical noise. An alternative interpretation of our results is that we have verified from quantum mechanics that the oscillatory dynamics of the field amplitudes in current SHG experiments are accurately described by classical mechanics.

The important contributions of B. Kennedy and P. Meystre to all aspects of this work are gratefully acknowledged. This work was supported in part by the National Science Foundation (NSF), Grant No. PHY-86-03368 and by the U.S. Joint Services Optics Program.

¹P. D. Drummond, K. J. McNeil, and D. F. Walls, *Opt. Acta* **27**, 321 (1980).

²H. J. Kimble and J. L. Hall, in *Quantum Optics IV*, edited by J. D. Harvey and D. F. Walls (Springer, Berlin, 1986).

³C. M. Savage and D. F. Walls, *Opt. Acta* **30**, 557 (1983).

⁴J. Ford, *Nature* **325**, 19 (1987).

⁵*Chaotic Behavior in Quantum Systems, Theory and Applications*, edited by G. Casati (Plenum, New York, 1985).

- ⁶P. D. Drummond and C. W. Gardiner, *J. Phys. A* **13**, 2353 (1980).
- ⁷P. D. Drummond, K. J. McNeil, and D. F. Walls, *Opt. Acta* **28**, 211 (1981).
- ⁸M. Dörfle and A. Schenzle, *Z. Phys. B* **65**, 113 (1986).
- ⁹M. Dörfle and R. Graham, in *Optical Instabilities*, edited by R. W. Boyd, M. G. Raymer, and L. M. Narducci (Cambridge University Press, Cambridge, England, 1986).
- ¹⁰R. Graham, *Phys. Scr.* **35**, 111 (1987).
- ¹¹R. Graham, *Phys. Rev. Lett.* **53**, 2020 (1984).
- ¹²R. Graham and T. Tel, *Phys. Rev. A* **31**, 1109 (1985).
- ¹³J. S. Satchell and S. Sarkar, *J. Phys. A* **19**, 2737 (1986); S. Sarkar and J. S. Satchell, *Phys. Rev. A* **33**, 2517 (1986); in *Nonlinear Phenomena and Chaos*, edited by S. Sarkar (Hilger, Bristol, 1986).
- ¹⁴D. F. Walls and G. J. Milburn, *Phys. Rev. A* **31**, 2403 (1985).
- ¹⁵M. Hillery, R. F. O'Connell, M. O. Scully, and E. P. Wigner, *Phys. Rep.* **106**, 121 (1984).
- ¹⁶E. B. Davies, *Quantum Theory of Open Systems* (Academic, New York, 1976), Sec. 3.4.
- ¹⁷G. J. Milburn, *Phys. Rev. A* **33**, 674 (1986).
- ¹⁸G. J. Milburn and D. F. Walls, *Am. J. Phys.* **51**, 1134 (1983).
- ¹⁹A. Yariv, *Quantum Electronics* (Wiley, New York, 1967).
- ²⁰R. Graham and T. Tel, *J. Stat. Phys.* **35**, 729 (1984).
- ²¹D. Ludwig, *SIAM Rev.* **17**, 605 (1975).
- ²²R. Kubo, K. Matsuo, and K. Kitahara, *J. Stat. Phys.* **9**, 51 (1973).
- ²³N. G. van Kampen, *Stochastic Processes in Physics and Chemistry* (North-Holland, Amsterdam, 1981).
- ²⁴P. Mandel and J. Erneux, *Opt. Acta* **29**, 7 (1982).
- ²⁵M. I. Friedlin and A. D. Wentzell, *Random Perturbations of Dynamical Systems* (Springer, New York, 1984).
- ²⁶D. F. Walls, *Nature* **306**, 141 (1983).
- ²⁷M. Collett and D. F. Walls, *Phys. Rev. A* **32**, 2887 (1985).
- ²⁸W. Zurek, *Phys. Rev. D* **24**, 1516 (1981); **26**, 1862 (1982).
- ²⁹W. E. Lamb, Jr., in Ref. 5.
- ³⁰P. Meystre and E. M. Wright, *Phys. Rev. A* (to be published).

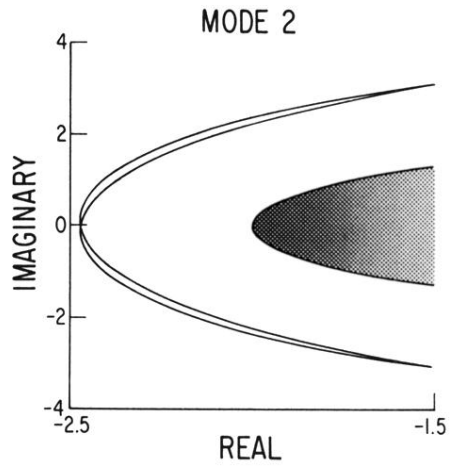


FIG. 1. Limit cycle of Eqs. (7), α_{2r} vs α_{2i} , defined by Eq. (6) as dimensionless scaled real and imaginary parts of the complex field amplitude of mode 2. Parameters: $E'=11.11$, $\Delta'_i=\Delta'_2=0$, $\gamma'=1$, period $\cong 2.312\gamma_1^{-1}$. Diffusion matrix \mathbf{D} is positive semidefinite only inside the shaded area. Note the different scales on the axes.